Korean J. Chem. Eng., **27**(5), 1391-1396 (2010)
DOI: 10.1007/s11814-010-0250-3

Laminar heat transfer of non-Newtonian nanofluids in a circular tube

Mohammad Hojjat, Seyed Gholamreza Etemad†, and Rohollah Bagheri

Department of Chemical Engineering, Isfahan University of Technology, Isfahan 84156-83111, Iran
(*Received 22 December 2009 • accepted 16 January 2010*)

Abstract−Forced convection heat transfer behavior of three different types of nanofluids flowing through a uniformly heated horizontal tube under laminar regime has been investigated experimentally. Nanofluids were made by dispersion of γ-Al_2O_3, CuO, and TiO_2 nanoparticles in an aqueous solution of carboxymethyl cellulose (CMC). All nanofluids as well as the base fluid exhibit shear-thinning behavior. Results of heat transfer experiments indicate that both average and the local heat transfer coefficients of nanofluids are larger than that of the base fluid. The enhancement of heat transfer coefficient increases by increasing nanoparticle loading. At a given Peclet number and nanoparticle concentration the local heat transfer coefficient decreases by axial distance from the test section inlet. It seems that the thermal entry length of nanofluids is greater than the base fluid and becomes longer as nanoparticle concentration increases.

Key words: Nanofluid, Non-Newtonian, Laminar Flow, Constant Wall Heat Flux, Heat Transfer, Nanoparticle

INTRODUCTION

One of the most important needs of modern industries is high performance heat transfer equipment. In the past few decades many techniques for heat transfer enhancement have been proposed. One idea involves improving the performance of heat transfer fluids by addition of solid particles [1]. Suspensions containing milli- or micro-sized particles have some problems, such as fast sedimentation, clogging of channels, high pressure drop, and severe erosion of system boundaries. Modern advances in material technologies provide the possibility of manufacturing particles of nanometer-sizes.

Stable suspensions of nano-sized (<100 nm) particles or fibers in conventional heat transfer fluids (such as water, ethylene glycol, and engine oil) were named nanofluid by Choi [2]. To understand and describe various features of flow and heat transfer behavior of nanofluids, numerous investigations were carried out [3]. Almost all previous investigations show that the thermal conductivity of nanofluids increases significantly over that of the base fluid [3-5].

Many investigators have studied the convective heat transfer of nanofluids. Oxide nanoparticles [6-21], carbon nanotubes [22,23] and some other types on nanoparticles [24-27] were used in preparation of nanofluids. Conventional heat transfer fluids such as water, ethylene glycol and transformer oil were employed as the base fluid. All investigators have studied convective heat transfer of nanofluids in circular tubes. Gherasim et al. [17], Nguyen et al. [10], and Farajollahi et al. [18] used a radial flow cooling system, a closed system designed for cooling of microprocessor or other electronic components and a shell and tube heat exchanger respectively. Both laminar [7-9,14-16,19-23,25] and turbulent [6,9-12,18,24,26-28] flow regimes were considered. Results of these investigations show that the heat transfer coefficient of nanofluids is considerably higher than that of the base fluid and the enhancement of heat transfer coefficient increases by nanoparticle concentration and nanofluid flow rate. Most of studies show that predicted values of conventional equations for heat transfer of single phase fluids are much smaller than experimental values of heat transfer coefficient of nanofluids. Enhancement of nanofluid thermal conductivity is one of the most important factors that improve nanofluid convective heat transfer. However, results of most studies indicate that the enhancement of the heat transfer coefficient of nanofluids is much higher than that solely attributed to the enhancement of thermal conductivity. Therefore, it is expected that other factors are also responsible for the convective heat transfer enhancement of nanofluids. Many review articles have described the factors affecting the enhancement of heat transfer of nanofluids in details [3,4,29-32].

Syam Sundar et al. [11] and Sharma et al. [28] have investigated convective heat transfer of nanofluids in plain tubes and tubes with twisted tape insert. Based on the results the heat transfer coefficient of nanofluids is greater than the base fluid and further enhancement achieved with twisted tape compared to that in a plain tube at the same conditions. Chandrasekar et al. [33] have shown that the enhancement of Nusselt number with inserted wire coil is larger than that of the plain tube. Results of Farajollahi et al. [18], Zeinali et al [8], Rea et al. [15] show that nanofluids have an optimum nanoparticle concentration at which the heat transfer enhancement reaches its maximum value. Some new correlations were proposed for the heat transfer of nanofluids [13,24].

Convective heat transfer characteristics of three types of non-Newtonian nanofluids containing γ-Al_2O_3, CuO, and TiO_2 in a horizontal circular tube with constant wall heat flux in laminar flow condition were studied experimentally. In the present investigation 0.5% wt. CMC solution was chosen as non-Newtonian base fluid. The difference between Newtonian and non-Newtonian nanofluids is that the base fluid of the former is a Newtonian fluid, while that of the later is a non-Newtonian fluid. Non-Newtonian fluids are widely used in many industries such as food, petrochemical, pharmaceutical industries, etc. Thus the behavior of non-Newtonian nanofluids could be useful to evaluate the possibility of heat transfer enhancement in various processes of these industries.

†To whom correspondence should be addressed.
E-mail: etemad@cc.iut.ac.ir

SAMPLE PREPARATION

By dispersing γ-Al_2O_3, TiO_2, and CuO nanoparticles in deionized water, three different types of nanofluids were prepared. The suspensions were subjected to ultrasonic vibration to obtain uniform suspensions, and then appropriate amounts of concentrated CMC solution were added to the suspension and mixed thoroughly with a mechanical mixer to achieve homogeneous nanofluids. Average sizes of γ-Al_2O_3, TiO_2 and CuO nanoparticles were 25, 10, and 30-50 nm, respectively.

To prevent possible sedimentation, for each test a new nanofluid was prepared and immediately used. Although no sedimentation was observed after several days of nanofluids preparation, in order to test the stability, in some cases, the density of samples of nanofluids was measured before and after test which no significant change in density was observed.

All nanofluids used in this investigation as well as the base fluid exhibited shear-thinning rheological behavior (n<1).

EXPERIMENTAL SETUP

To investigate the convection heat transfer of nanofluids in a horizontal uniformly heated circular tube, an experimental apparatus was designed and constructed (shown schematically in Fig. 1). The experimental setup consists of a flow loop, a cooling unit, and measuring and control units. The flow loop included a stainless steel gear pump, a nanofluid holding tank, a bypass line, a flow meter, a calming chamber, a test section, a mixing chamber and several valves. A straight stainless steel (type 316) tube of 2,110-mm length, 10 mm inner diameter, and 14 mm outer diameter was used as the test section. To obtain constant wall heat flux boundary conditions, the test section was electrically heated by an adjustable DC power supply with maximum power of 10 kW. To measure the wall temperatures, ten K-type thermocouples were mounted on the tube by an epoxy adhesive with high thermal conductivity at axial positions of 100, 150, 200, 350, 550, 800, 1,100, 1,400, 1,700, and 2,000 mm from the test section inlet. To reduce the heat loss from the test section it was thermally insulated from the upstream and downstream sections by thick Teflon bushings. Two K-type thermocouples were also inserted in the calming chamber and the mixing chamber to measure the inlet and outlet bulk temperatures of the nanofluid, respectively. The whole test section including the calming and mixing chambers was heavily insulated. Flow rates were measured by a magnetic flow meter (WELLTECH COPA-XE WT4300, China) with precision of 0.1 percent. A double pipe cooler was used to adjust the inlet bulk temperature of the nanofluids at the desired value.

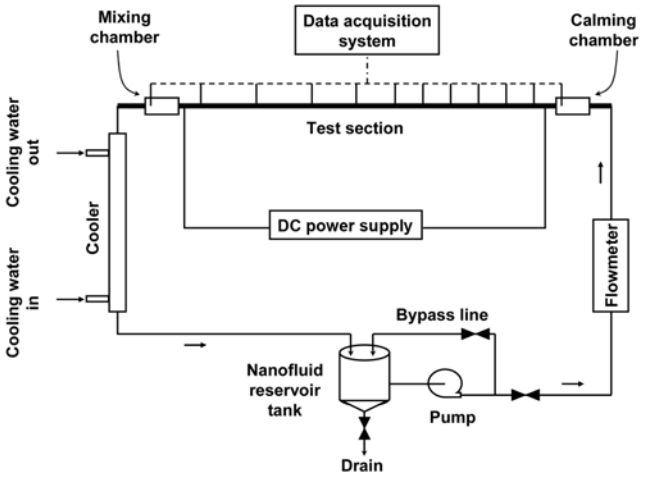

Fig. 1. Schematic diagram of the experimental setup.

DATA ANALYSIS

The wall heat flux is calculated as follows:

$$q'' = \frac{mC_P(T_{b2} - T_{b1})}{\pi DL} \tag{1}$$

T_{b1} and T_{b2} are tube inlet and outlet fluid bulk temperatures, respectively.

The wall heat flux can also be calculated as follows:

$$q'' = \frac{VI}{\pi DL} \tag{2}$$

where V is electrical potential difference applied to tube wall and I is electrical current flowing through the tube wall.

Average difference between values calculated by these two equations is about 5 percent, which can be due to the heat loss through the tube to surroundings.

The local heat transfer coefficient at each axial position is calculated by the following equation:

$$h_z = \frac{q''}{T_{wi} - T_b} \tag{3}$$

T_b is the bulk temperature at axial position and is calculated as follows:

$$T_b = T_{b1} + (T_{b2} - T_{b1})\frac{z}{L} \tag{4}$$

Inner wall temperature at each axial position, T_{wi}, is calculated from the following equation [34]:

$$T_{wi} = T_{wo} + \frac{q}{4k_s}(r_o^2 - r_i^2) - \frac{q}{2k_s} r_o^2 \ln\frac{r_o}{r_i} \tag{5}$$

where T_{wo} is outer wall temperature, q is heat generation per unit volume of tube, r_i and r_o are tube inner and outer diameter, respectively, and k_s is tube wall thermal conductivity.

The local Nusselt number is calculated as follows:

$$Nu_z = \frac{h_z \cdot D}{k} \tag{6}$$

Average heat transfer coefficient is calculated by the following equation [35]:

$$h = \frac{1}{L}\int h_z dz = \frac{1}{L}\sum_{k=1}^{N_{TC}} h_{zk}\Delta z_k \tag{7}$$

where N_{TC} is the number of thermocouples and Δz_k is shown in Fig. 2.

Average Nusselt number is calculated as:

$$Nu = \frac{h \cdot D}{k} \tag{8}$$

All nanofluids employed in this study exhibit the power-law rheo-

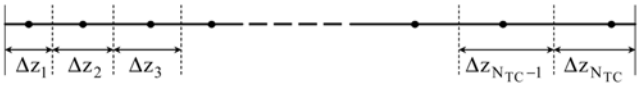

Fig. 2. Parameters of Eq. (7).

logical behavior expressed by the following equation:

$$\tau = K\gamma \tag{9}$$

For purely viscous non-Newtonian fluid, the Reynolds number is defined as follows:

$$Re = \frac{\rho \cdot u^{2-n} \cdot D^n}{K} \tag{10}$$

The nanofluid thermal conductivity (k_{nf}) and the rheological parameters (n and K) of the power-law model were determined from experimental measurements [36,37]. Other physical properties of nanofluids were calculated from the base fluid and nanoparticle properties at the average bulk temperature by using the following correlations [6,38]:

$$\rho_{nf} = \phi\rho_p + (1-\phi)\rho_{bf} \tag{11}$$

$$(\rho C_P)_{nf} = \phi(\rho C_P)_p + (1-\phi)(\rho C_P)_{bf} \tag{12}$$

The thermocouples were calibrated with a precision of 0.1 ºC. The flow rate was measured with a maximum error of 0.1 percent. Therefore, the uncertainty of the convective heat transfer coefficient of nanofluids in all cases is estimated to be less than 5.2 percent.

EXPERIMENTAL RESULTS AND DISCUSSION

To evaluate the accuracy and reliability of the experimental data, measurements were first carried out using de-ionized water as the working fluid for which good correlations exist in literature. The Nusselt numbers calculated using the experimental data were compared with the Nusselt numbers predicted by the Shah equation for laminar flow [39]:

$$Nu = \begin{cases} 1.953\left(RePr\frac{D}{x}\right) & \left(RePr\frac{D}{x}\right) \geq 33.3 \\ 4.364 + 0.0722RePr\frac{D}{x} & \left(RePr\frac{D}{x}\right) < 33.3 \end{cases} \tag{13}$$

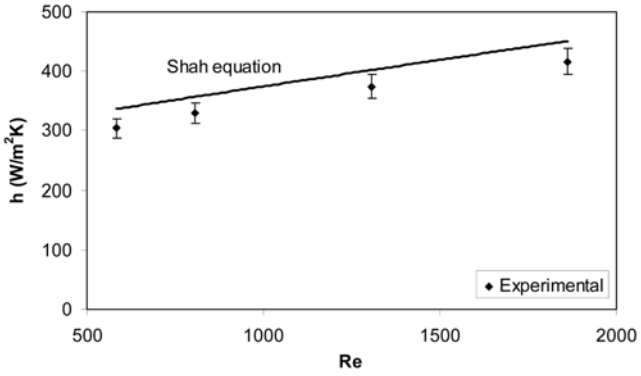

Fig. 3. Heat transfer coefficient of deionized water vs. Reynolds number.

Results of this comparison are presented in Fig. 3. Maximum and average difference between experimental data and those predicted by the Shah equation is 9.4 and 8 percent, respectively. Thus, there exists very good agreement between the results of the present study and those predicted by the Shah equation.

In Fig. 4(a)-(c) the average heat transfer coefficient of nanofluids is plotted as a function of Peclet number at different nanoparticle concentrations. It is clear that addition of nanoparticles to the base fluid enhances its heat transfer coefficient significantly. For example, at a Peclet number of about 50,000 the heat transfer coefficients of γ-Al_2O_3, TiO_2 and CuO nanofluids are 17.7, 16.1, and 19.3 percent greater than those of the base fluid, respectively. At a certain Peclet number enhancement of heat transfer coefficient increases by increasing nanoparticle concentration. For example, at a Peclet

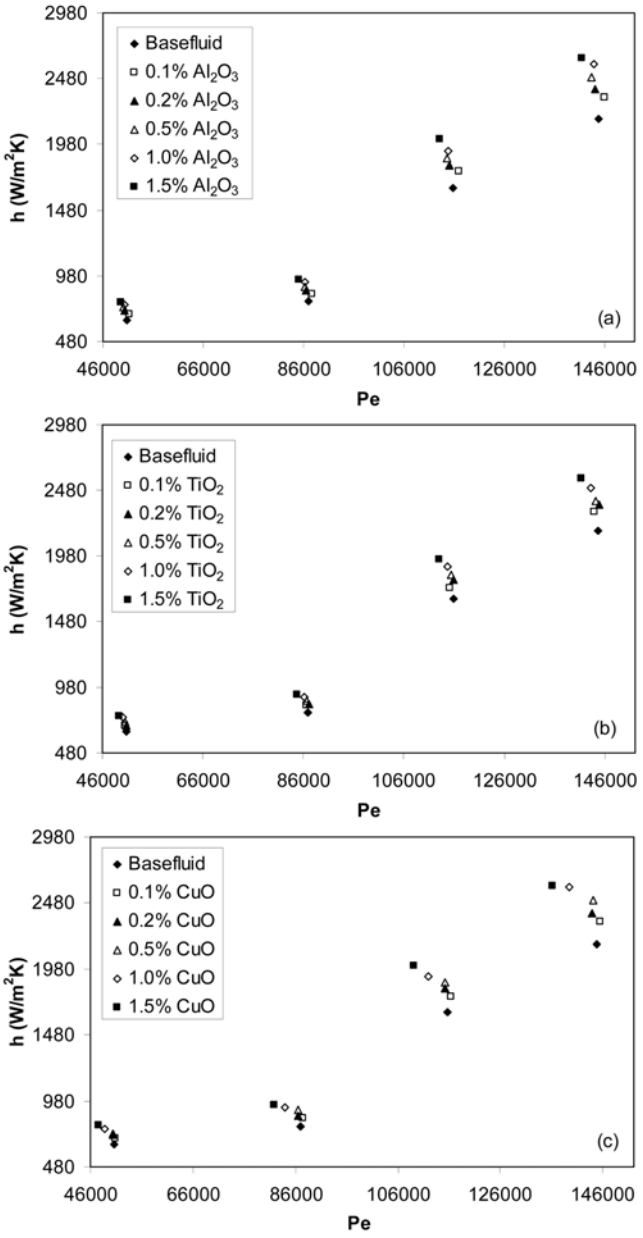

Fig. 4. (a)-(c) Average heat transfer coefficient of nanofluids as a function of Peclet number.

number of about 140,000, by increasing of nanoparticle loadings from 0.1 to 1.5% by volume, the enhancement of heat transfer coefficients of γ-Al_2O_3, TiO_2 and CuO nanofluids increases from 7.4, 6.7, and 7.9 to 21.3, 18.4, and 21.2 percent, respectively. At given nanoparticle concentration the heat transfer coefficient of nanofluids increases with increasing Peclet number.

Similar trends were observed for the Nusselt number of nanofluids, i.e., the Nusselt number of nanofluids increases with nanoparticle concentration and Peclet number in the same manner.

Enhancement of the effective thermal conductivity is an important factor that causes the increase of the convective heat transfer coefficient of nanofluids. But based on the results the enhancement of the heat transfer coefficient of nanofluids is much more than that attributed to the thermal conductivity enhancement. This shows that some other factors contribute in the enhancement of the heat transfer coefficient. The local heat transfer coefficient, h, can be approximately given as k/δ_t with δ_t the thickness of thermal boundary layer [19]. This means that enhancement of thermal conductivity of nanofluids and/or decreasing thermal boundary layer thickness increases the heat transfer coefficient. Since the enhancement of the heat transfer coefficients is larger than the effect of thermal conductivity enhancement, it seems that the thermal boundary layer thickness of nanofluids is smaller than that of the base fluid. This may be due to the non-Newtonian behavior of nanofluids. For pseudoplastic fluids, because the shear rate close to the wall is large, the apparent viscosity is small, which leads to a smaller boundary layer thickness. The thermal dispersion due to the inherent random motion of particles also contributes to this enhancement, which, in turn, results in a flat temperature profile. As a result, the temperature gradient at the wall becomes steeper and the heat transfer rate at the wall increases [24,38,40]. Some other factors such as thermophoresis, collision of nanoparticles and slip velocity between the fluid and nanoparticles could also be responsible for the heat transfer coefficient enhancement.

Relative heat transfer coefficient of nanofluids as a function of Peclet number is shown in Fig. 5. It is observed that the Peclet number has no significant influence on the enhancement of heat transfer coefficient of nanofluids. That is, the heat transfer coefficient of nanofluids and those of the base fluid are enhanced by the same ratio. Similar behavior was reported by other investigators [6,25].

The local heat transfer coefficient of nanofluids as a function of axial distance from inlet of test section at different nanoparticle concentration for Peclet number of about 140,000 is shown in Fig. 6. At a given Peclet number and axial distance from tube inlet, the local heat transfer coefficient of nanofluids increases with increase in nanoparticle concentration. For example, at a Peclet number of about 140000 and axial position of 500 mm (z/L=0.26) the local heat transfer coefficients of γ-Al_2O_3, TiO_2 and CuO nanofluids with nanoparticle concentration of 0.1 and 1.0% by volume are (4.9%, 6.7%, 7.6%) and (15.9%, 13.0%, 19.0%) larger than those of the base fluid, respectively. At a certain Peclet number and nanoparticle concentration the local heat transfer coefficient of nanofluids decreases with increase in axial distance. For example, as nanofluids flow from tube inlet to tube exit at Peclet number of about 140000, the local heat transfer coefficients of γ-Al_2O_3, TiO_2 and CuO with 0.5% vol. nanoparticle concentration, decrease by 21.3, 21.8, and 26.4 percent, respectively. This is due to the increasing boundary

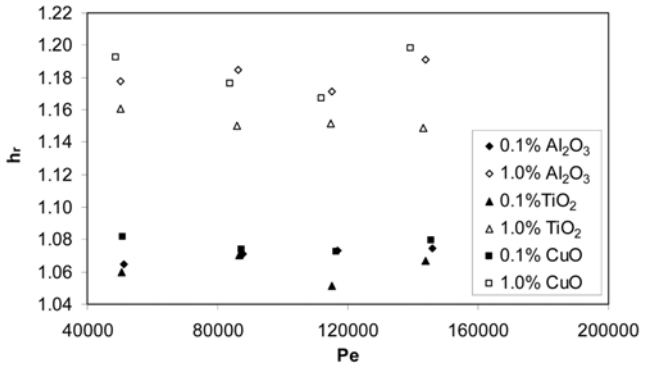

Fig. 5. Relative heat transfer coefficient of nanofluids as a function of Peclet number.

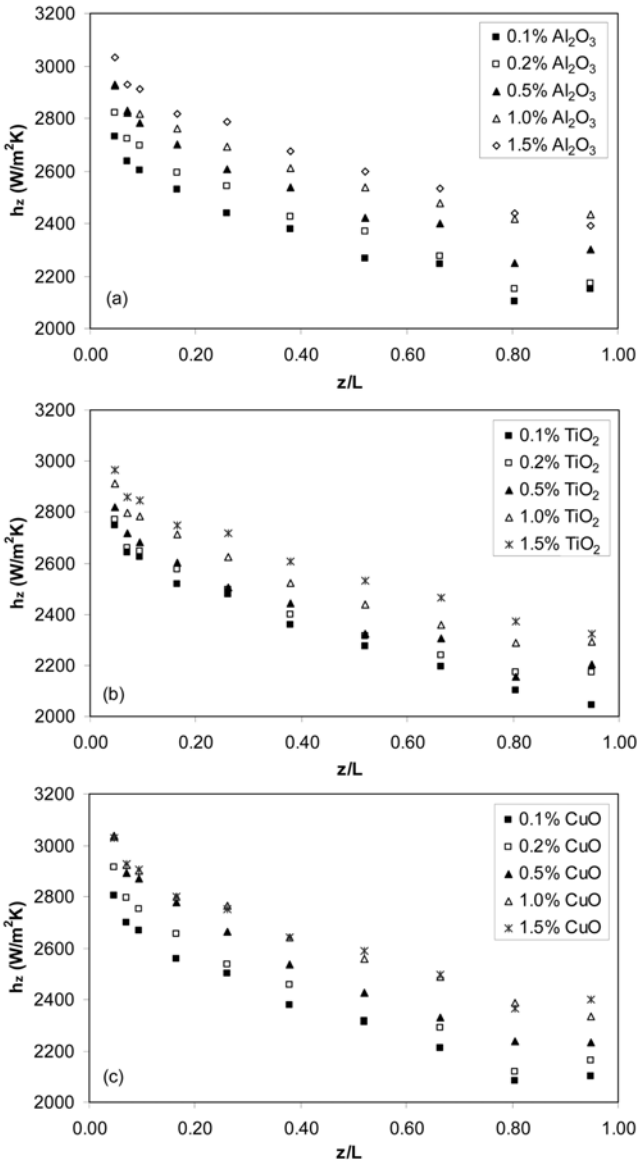

Fig. 6. (a)-(c) Local heat transfer coefficient of nanofluids as a function of axial distance from tube inlet.

layer thickness with increase in axial distance.

It seems that the entrance region for nanofluids is longer than that of the base fluid, and increases by increasing nanoparticle concentration. This is due to decreasing thermal boundary layer thickness of nanofluids relative to that of the base fluid.

CONCLUSIONS

Convective heat transfer characteristics of suspensions including three different nanoparticles (γ-Al_2O_3, TiO_2 and CuO) in an aqueous solution of CMC flowing through a uniformly heated horizontal tube were investigated experimentally. The following observations were made:

- The average heat transfer coefficient of nanofluids is larger than that of the base fluid. The enhancement of heat transfer coefficient increases with an increase in the Peclet number and the nano- particle concentration.
- The convective heat transfer enhancement of nanofluids is much more than the effect of the thermal conductivity enhancement. This implies that some other factors such as thermophoresis, nanoparticles thermal dispersion, decreasing thermal boundary layer thickness, migration of nanoparticles, and nanofluid viscosity influence the convection heat transfer coefficient. Identification of the impact of these factors requires further investigations.
- Relative heat transfer coefficients for all three types of nanofluids increase with an increase in the nanoparticle concentration. The Peclet number has no significant effect on relative heat transfer coefficient. Some previous researchers have also reported similar behavior.
- At a certain Peclet number and axial position, the local heat transfer coefficient of nanofluids increases with increasing nanoparticle concentration.
- At a given Peclet number and nanoparticle concentration the local heat transfer coefficient of nanofluids as well as the base fluid decreases with increasing axial distance from the inlet of the test section.

ACKNOWLEDGEMENT

This work was partially supported by the Petrochemical Research and Technology Company in I. R. Iran.

NOMENCLATURE

A : heat transfer area [m^2]
C_P : heat capacity [kJ/kg K]
D : tube internal diameter [m]
h : average heat transfer coefficient [W/m^2K]
h_r : relative heat transfer coefficient (dimensionless)
h_z : local heat transfer coefficient [W/m^2K]
I : electrical current [A]
k : thermal conductivity [W/m K]
K : consistency index [Pa s^n]
L : tube length [m]
m : mass flow rate [kg/s]
n : power law index (dimensionless)
Nu : local nusselt number (dimensionless)
$\overline{Nu}$: average nusselt number (dimensionless)
q″ : wall heat flux [W/m^2]
q : heat generation per unit volume [W/m^3]
Pr : prandtl number (dimensionless)
Pe : peclet number (dimensionless)
r : tube radius [m]
Re : reynolds number (dimensionless)
Re_{MR} : metzner-reid reynolds number (dimensionless)
T : temperature [K]
T_{b1} : inlet bulk temperature of fluid [K]
T_{b2} : outlet bulk temperature of fluid [K]
u : fluid average velocity [m/s]
V : electrical potential; difference [V]
z : axial distance from tube inlet [m]

Greek Symbols

ϕ : particle volume concentration (dimensionless)
γ : shear rate [1/s]
ρ : density [kg/m^3]
τ : shear stress [Pa]

Subscript

b : bulk
bf : base fluid
i : inner
nf : nanofluid
o : outer
p : particle
w : wall

REFERENCES

1. J. C. Maxwell, *Electricity and magnetism*, Clarendon Press, Oxford, U.K. (1873).
2. S. U. S. Choi, in *American Society of Mechanical Engineers*, Fluids Engineering Division (Publication) FED, **231**, 99 (1995).
3. L. Godson, B. Raja, D. Mohan Lal and S. Wongwises, *Renew. Sustainable Energy Rev.*, **14**(2), 629 (2009).
4. W. Yu, D. M. France, J. L. Routbort and S. U. S. Choi, *Heat Transf. Eng.*, **29**(5), 432 (2008).
5. Y. Li, J. Zhou, S. Tung, E. Schneider and S. Xi, *Powder Technol.*, **196**(2), 89 (2009).
6. B. C. Pak and Y. I. Cho, *Exp. Heat Transf.*, **11**, 151 (1998).
7. D. Wen and Y. Ding, *Int. J. Heat Mass Transf.*, **47**, 5181 (2004).
8. S. Z. Heris, S. G. Etemad and M. N. Esfahany, *Int. Commun. Heat Mass Transf.*, **33**(4), 529 (2006).
9. Y. He, Y. Jin, H. Chen, Y. Ding, D. Cang and H. Lu, *Int. J. Heat Mass Transf.*, **50**(11-12), 2272 (2007).
10. C. T. Nguyen, G. Roy, C. Gauthier and N. Galanis, *App. Therm. Eng.*, **27**(8-9), 1501 (2007).
11. L. Syam Sundar, K. V. Sharma and S. Ramanathan, *Int. J. Nanotech. Appl.*, **2**, 21 (2007).
12. D. P. Kulkarni, P. K. Namburu, H. E. Bargar and D. K. Das, *Heat Transf. Eng.*, **29**(12), 1027 (2008).
13. K. V. Sharma, L. S. Sundar and P. K. Sarma, *Int. Commun. Heat Mass Transf.*, **36**(5), 503 (2009).
14. K. B. Anoop, T. Sundararajan and S. K. Das, *Int. J. Heat Mass Transf.*, **52**(9-10), 2189 (2009).
15. U. Rea, T. McKrell, L. W. Hu and J. Buongiorno, *Int. J. Heat Mass*

Transf., **52**(7-8), 2042 (2009).
16. K. S. Hwang, S. P. Jang and S. U. S. Choi, *Int. J. Heat Mass Transf.*, **52**(1-2), 193 (2009).
17. I. Gherasim, G. Roy, C. T. Nguyen and D. Vo-Ngoc, *Int. J. Therm. Sci.*, **48**(8), 1486 (2009).
18. B. Farajollahi, S. Gh. Etemad and M. Hojjat, *Int. J. Heat Mass Transf.*, **53**(1-3), 12.
19. W. Y. Lai, S. Vinod, P. E. Phelan and P. Ravi, *J. Heat Transf.*, **131** (11), 112401 (2009).
20. M. Chandrasekar, S. Suresh and A. Chandra Bose, *Exp. Therm. Fluid Sci.*, **34**(2), 122 (2010).
21. B. H. Chun, H. U. Kang and S. H. Kim, *Korean J. Chem. Eng.*, **25**(5), 966 (2008).
22. Y. Ding, H. Alias, D. Wen and R. A. Williams, *Int. Commun. Heat Mass Transf.*, **49**, 240 (2006).
23. P. Garg, J. L. Alvarado, C. Marsh, T. A. Carlson, D. A. Kessler, and K. Annamalai, *Int. J. Heat Mass Transf.*, **52**(21-22), 5090 (2009).
24. Y. Xuan and Q. Li, *J. Heat Transf.*, **125**(1), 151 (2003).
25. Y. Yang, Z. G. Zhang, E. A. Grulke, W. B. Anderson and G. Wu, *Int. J. Heat Mass Transf.*, **48**(6), 1107 (2005).
26. W. Yu, D. M. France, D. S. Smith, D. Singh, E. V. Timofeeva, and J. L. Routbort, *Int. J. Heat Mass Transf.*, **52**(15-16), 3606 (2009).
27. S. Torii and W.-J. Yang, *J. Heat Transf.*, **131**, (2009).
28. A. Sharma and S. Chakraborty, *Int. J. Heat Mass Transf.*, **51**(19-20), 4875 (2008).
29. J. M. Laskar, J. Philip and B. Raj, *Phys. Rev. E - Statistical, Nonlinear, and Soft Matter Physics*, **78**(3), (2008).
30. X.-Q. Wang and A. S. Mujumdar, *Int. J. Therm. Sci.*, **46**, 1 (2007).
31. X.-Q. Wang and A. S. Mujumdar, *Brazilian J. Chem. Eng.*, **25**(4), 631 (2008).
32. S. Kakaç and A. Pramuanjaroenkij, *Int. J. Heat Mass Transf.*, **52** (13-14), 3187 (2009).
33. M. Chandrasekar, S. Suresh and A. Chandra Bose, *Exp. Therm. Fluid Sci.*, **34**(2), 210 (2010).
34. F. P. Incropera and D. P. DEWitt, *Fundamentals of heat and mass transfer*, Fourth Ed., John Wiley & Sons, New York (1996).
35. M. Kutz, *Heat transfer calculations*, McGraw-Hill, New York, NY (2006).
36. M. Hojjat, S. Gh. Etemad, R. Bagheri and J. Thibault, in *8th World Congress of Chemical Engineering*, Montreal, Canada (2009).
37. M. Hojjat, S. Gh. Etemad, R. Bagheri and J. Thibault, in *The 6th Int. Chemical Engineering Congress & Exhibition*, Kish Island, Iran (2009).
38. Y. Xuan and W. Roetzel, *Int. J. Heat Mass Transf.*, **43**(19), 3701 (2000).
39. R. K. Shah, in *3rd National Heat and Mass Transf.*, Indian Institute of Technology, Bombay, India, **1**, HTM (1975).
40. S. Z. Heris, M. N. Esfahany and G. Etemad, *Numer. Heat Transf. Part A*, **52**(11), 1043 (2007).